GI_Forum 2023, Issue 1
Page: 22 - 33
Full Paper
Corresponding Author:
igitas@for.auth.gr
DOI: 10.1553/giscience2023_01_s22

Above-Ground Forest Biomass Estimation using Multispectral LiDAR Data in a Multilayered Coniferous Forest

Nikos Georgopoulos[1], Konstantinos Antoniadis[1], Michail Sismanis[1], Ioannis Gitas[1]
[1]Aristotle University of Thessaloniki, Greece

Abstract

Above-ground biomass and carbon stock are fundamental components of the global carbon cycle, essential for climate change mitigation. Remote sensing data can provide timely and accurate estimates of various forest attributes, especially over large and remote forested areas. The objective of this research was to investigate the potential of multispectral LiDAR data for estimating the stem biomass (SB) and total biomass (TB) in a multi-layered fir forest using an Edge-tree corrected Area Based Approach (EABA). Subsequently, a Random Forest (RF) regression analysis was performed to develop SB and TB predictive models using LiDAR-derived height metrics. Two RF models were produced and evaluated in terms of their predictive performance. Overall, our work demonstrates the capability of multispectral LiDAR data to provide reliable SB and TB estimates in a complex structured forest, contributing significantly to sustainable forest management.

Keywords:

forest biomass, multispectral LiDAR, remote sensing

1 Introduction

Forests are a key component of the terrestrial carbon cycle, providing various socio-economic and environmental services (Cao, Liu, Shen, Wu & Liu, 2019). Plants store more than 80% of the total above-ground carbon, while at the same time removing large amounts of CO_2 from the atmosphere (Węgiel & Polowy, 2020). Forest biomass consists of various components (stems, leaves, needles, branches, bark, roots) and can be classified into above-ground biomass (AGB) and below-ground biomass, commonly expressed as the dry mass at the individual tree level (Kajimoto et al., 1999; Luo et al., 2017). Traditionally, field measurements are required to estimate AGB, which in most cases involve destructive sampling, diameter at breast height (DBH) measurements, and tree height (Zhang Z., Cao & She, 2017) – direct measurements that are considered laborious and time-consuming (Dutcă et al., 2020).

In recent decades, various remote sensing technologies have been applied for biomass estimation (Wang & Jiao, 2020). While a variety of remote sensors have been employed for

forest biomass estimation (e.g. Multispectral and Hyperspectral Optical sensors, Synthetic Aperture Radar sensors), Light Detection and Ranging (LiDAR) has been identified as the most accurate data source for forest parameters and biomass estimation (Clark, 2011; Socha et al., 2020). LiDAR instruments have become the dominant sensors for accurate AGB estimation, mostly due to their ability to penetrate the forest canopy, providing 3D information for all forest layers (Jiang, Li, Lu, Chen & Wei, 2020; Silva Carlos A. et al., 2016).

Recent developments in LiDAR technology have led to the development of multispectral systems. The latest LiDAR sensors have the ability to gather vertical distribution information on different physiological processes across multiple spectral channels (Wallace, Nichol & Woodhouse, 2012). The additional, complementary, information derived from multispectral LiDAR data has been widely used in studies for improved land-cover and biomass estimation (Dalponte, Ene, Gobakken, Næsset & Gianelle, 2018; Georgopoulos, Gitas, Stefanidou, Korhonen & Stavrakoudis, 2021; Hopkinson, Chasmer, Gynan, Mahoney & Sitar, 2016). According to these studies, the AGB is highly correlated with the mean intensity values of the multispectral LiDAR data for the various forest layers.

AGB quantification can be accomplished using either single-tree or plot-level approaches. The former usually aims to extract height- and/or intensity-derived metrics for each individual tree (Latella, Sola & Camporeale, 2021). However, the single-tree approach requires high pulse densities and its effectiveness is closely related to the accuracy of tree detection and of the crown delineation (Georgopoulos et al., 2021). Biomass estimates at the plot level, on the other hand, have been widely used in different biomes (Kelley, Trofymow, Metsaranta, Filipescu & Bone, 2021; Næsset, 2004; Silva Carlos Alberto et al., 2018) and include the integration of height-derived and other LiDAR-related metrics to predict forest characteristics. It should be noted that the plot-level approach provides more accurate AGB and carbon estimates compared to the tree-level approach, mostly due to the poor performance of the segmentation algorithms used to identify the understorey trees (Coomes et al., 2017). For the task of estimating AGB, various regression methods have been tested along with LiDAR data. These include linear regression (Salum et al., 2020), Support Vector Machines (Almeida et al., 2019), Random Forest (Sun, Li, Wang & Fan, 2019), Extreme Gradient Boosting (Li, Li, Li & Liu, 2019), Artificial Neural Networks (Dong, Tang, Min, Veroustraete & Cheng, 2019), and deep learning models (L. Zhang, Shao, Liu & Cheng, 2019).

Although many different biomes and tree species have been adequately examined in the literature, few studies have explored the potential of LiDAR remote sensing for estimating the biomass of multilayered forests (Dorado-Roda et al., 2021; Korpela, Hovi & Morsdorf, 2012). The purpose of this study is to assess the potential of multispectral LiDAR data in estimating both stem biomass (SB) and total biomass (TB) in a multilayered fir forest in central Greece. More specifically, the Random Forest regression algorithm was examined using LiDAR-derived height-related metrics to investigate its potential for achieving reliable estimates of SB and TB.

2 Materials and Methods

2.1 Study Area

The study area is located in the southeastern part of Mt. Pindos in Pertouli, Greece, and covers almost 33 km² (Figure 1). The mountainous forest has been under the management of the Aristotle University of Thessaloniki since 1934 for research and education purposes. The climate in the area is transitional Mediterranean to Mid-European, exhibiting significant variations across seasons. The dominant tree species in the study area is *Abies borissi regis* (Bulgarian fir), with individual trees of Scots pine and black pine, and various broadleaf species (e.g., beech, Austrian oak, various willow species, English yew and maple). The forest stands consist of different-aged trees, including mature fir trees in the overstorey, as well as natural regeneration and young trees in the understorey.

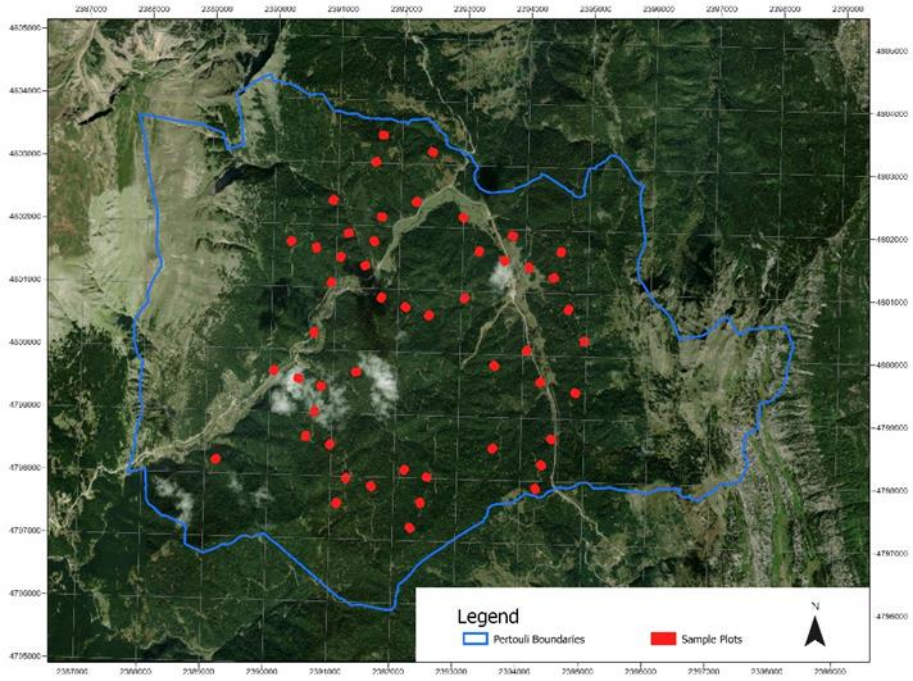

Figure 1: Map of the study area, including the forest boundaries and plots, projected in WGS 84.

2.2 Dataset Description

Field data

Field measurements were conducted in 2019 and 2022, with a total of 48 pure Bulgarian fir plots in Pertouli University Forest being measured in both campaigns. Plots were located using

a handheld GPS with an average horizontal positional accuracy of 3m and covering a total area of 1000 m^2. In each plot, the DBH and height of all trees were extracted from the forest inventory plan, completed in 2018.

LiDAR Data

Multispectral LiDAR data for Pertouli University Forest were acquired in 2018. Data collection used a RIEGL VQ-1560i-DW laser scanner sensor mounted on an airplane. The data included information derived from two spectral channels, namely Green and Near Infrared (532 nm and 1064 nm, respectively). All data collected were preprocessed by the provider, resulting in a dense point cloud (maximum of 7 returns per pulse). The mean point cloud density of all acquisitions is 82.99 points m^{-2}, with a scan angle range of -32° to $+32^\circ$.

2.3 LiDAR Analysis

LiDAR data processing was performed primarily using R and more specifically the lidR package (R Core Team, 2017; Roussel et al., 2020). First, the point cloud covering each plot was extracted and height-normalized using the kriging algorithm (Oliver & Webster, 1990). Large scan angles (i.e. greater than $\pm 15^\circ$) were removed to avoid errors originating from off-nadir angles, which have a significant impact on the LiDAR-derived canopy structure metrics (Donoghue, Watt, Cox & Wilson, 2007). Subsequently, the pit-free algorithm was employed for the generation of the canopy height model (CHM), since it provides significantly improved tree detection accuracy in high-density LiDAR data (Khosravipour, Skidmore, Isenburg, Wang & Hussin, 2014). Tree segmentation was performed using the watershed algorithm and the CHM.

In this study, an Edge-tree corrected Based Approach (EABA) was implemented. Thus the tree crowns obtained from the segmentation process were used to adjust the plot boundaries (Kotivuori, Maltamo, Korhonen, Strunk & Packalen, 2021) (Figure 2). According to Packalen, Strunk, Pitkanen, Temesgen & Maltamo (2015), this approach provides lower Relative Mean Square Error (RMSE) for the stem volume prediction compared to the traditional Area Based approach. In addition, the EABA can minimize the effects of co-registration errors, which are frequent in the typical plot-based approach (Pascual, 2019).

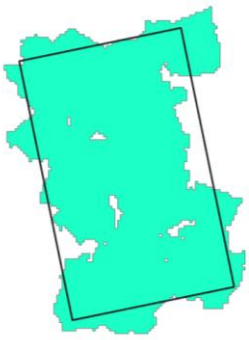

Figure 2:
Plot footprint for the EABA approach. The black rectangle represents the corrected plot where the height metrics were calculated.

Finally, a suite of LiDAR-derived height metrics were calculated, an overview of which is presented in Table 1.

Table 1: LiDAR-derived metrics calculated for the SB and TB estimation. All metrics were calculated excluding the ground returns.

LiDAR Metrics	Description
p10, p20… p95, p99	Height Percentiles
b10, b20… b95, b99	Height Bicentiles
Hmax	Max Height
Havg	Average Height
Hstd	Height Standard Deviation
Hskew	Height Skewness
Hkur	Height Kurtosis
Hqav	Average Square Height

2.4 Biomass Estimation using Allometric Equations

The reference SB and TB were calculated using species-specific allometric equations developed by Georgopoulos et al. (2021). More specifically, these equations were developed using ordinary least square regression from 32 destructively sampled trees and were based primarily on DBH (Table 2). The SB includes the stem and bark biomass, while the TB includes all the above-ground biomass components (stem, bark, needles and branches).

Table 2: Parameter values, residual standard error, R2, and adjusted R2 for total stem and total biomass estimation of the allometric equations based on DBH.

Equation	Parameter	RSE	R2	adjR2
Stem Biomass	a = 8.3488 b = 2.5691	0.3014	0.9597	0.9584
Total Biomass	a = 8.63722 b = 2.46266	0.1563	0.9913	0.9905

2.5 Regression model and accuracy assessment

In this study, the Random Forest (RF) algorithm was examined for its potential to reliably predict both TB and SB. Prior to the statistical analysis, all the predictors (i.e., reference data) were 'Centre'-scaled and divided into two sets, namely training (70%) and testing (30%) sets. Additionally, a nested ten-fold cross-validation was applied in each training set to obtain the best-performing model. The regression models were validated using an independent testing

set (30% of the total number of samples), which was randomly split from the training data to obtain the predictive performance of each algorithm. Assessment of the models' performance for SB and TB estimation was based on the Mean Absolute Error (MAE), bias, Relative Mean Square Error (RMSE), and R^2.

3 Results

SB and TB were estimated using the RF algorithm, and the RF was evaluated for its potential to reliably estimate both. The results are presented in detail in the following sections.

3.1 Stem Biomass

The performance of the RF for the SB estimate when multispectral LiDAR data are used is presented in Table 3. The model fit is illustrated in Figure 3, which shows the regression line and the confidence interval. Concerning the model's tuning, the number of trees to be grown was set at 300 (according to the grid-search and cross- validation results), and the number of variables was set as the number of predictors divided by three.

In general, the RF model achieved a reasonable prediction rate, with an R^2 of 0.71. More specifically, the RF model developed in this project provided satisfactory results in terms of MAE (2175.80 kg/1000 m^2), rbias (-0.21), and RMSE% (27.69%).

Table 3: Testing the performance of the algorithm for stem biomass (SB) estimation using multispectral LiDAR data.

Model	MAE	rbias	RMSE	RMSE %	R^2
RF	2,175.80	-0.21	2,661.46	27.69	0.71

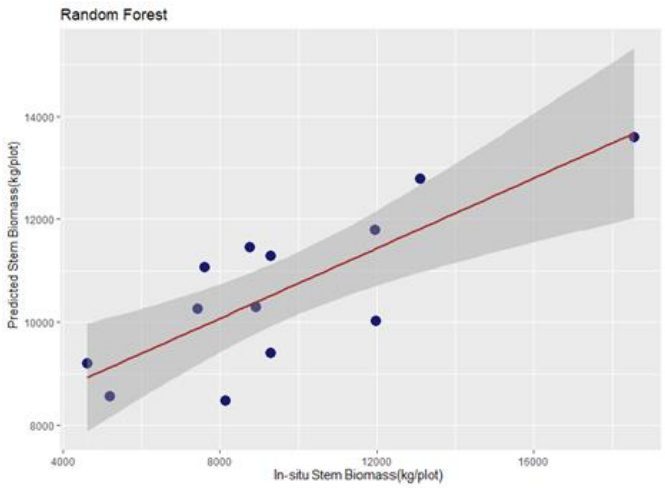

Figure 3: Scatterplots of the observed versus the predicted stem biomass (SB).

3.2 Total Biomass

The performance of the RF for TB estimation using multispectral LiDAR data is presented in Table 4. The model fit is illustrated in Figure 34. In this instance, the number of trees to be grown was set to 100 (according to the grid-search and cross-validation results); the number of variables was set as the number of predictors divided by three, as for the SB model.

In general, the RF model achieved an R^2 of 0.76 on the testing set, which is slightly higher than for the SB model. In addition, the MAE is higher than for the SB model (i.e., 2593.56 kg/1000 m^2). As far as the RMSE and bias are concerned, the results were noticeably improved (-0.05 and 24.67% respectively).

Table 4: Testing the performance of the algorithm for total biomass (TB) estimation using multispectral LiDAR data.

Model	MAE	rbias	RMSE	RMSE %	R^2
RF	2593.56	-0.05	3561.10	24.67	0.76

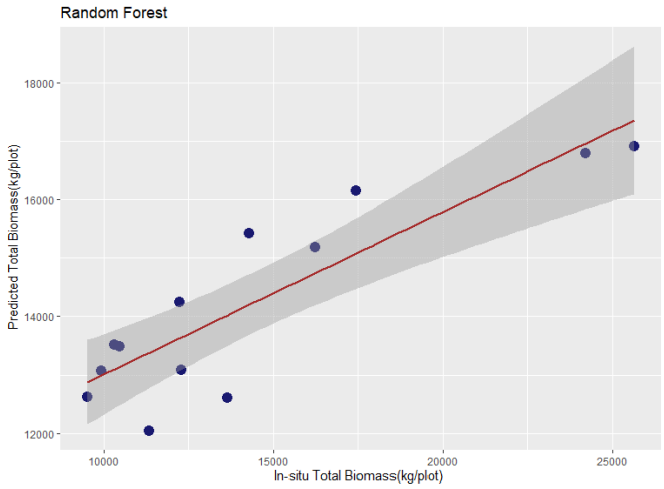

Figure 4: Scatterplots of the observed versus the predicted total biomass (TB).

4 Discussion

In this study, multispectral LiDAR data were evaluated for their potential in reliably estimating SB and TB in a multilayered coniferous forest. More specifically, height-related LiDAR-derived metrics were used as inputs to an RF regression algorithm to estimate EABA, SB and TB in 48 sample plots. A set of species-specific allometric equations were used to extract reference values for SB and TB in each plot.

Overall, the results demonstrate that both SB and TB can be accurately estimated using LiDAR data and the RF algorithm in a structured forest with trees of different ages. In the case of the SB, the results are in accordance with most published studies that have analysed LiDAR data in different ecosystems (e.g., Allouis, Durrieu, Vega & Couteron, 2013; Cao, Coops, Innes, Dai & She, 2014; Cao et al., 2019; Georgopoulos et al., 2021). Thus, we can consider that SB is well described by the LiDAR-derived height-related metrics. The TB model's estimation accuracy was slightly better than the SB one, a finding similar to that of Cao et al. (2014). The results show that the TB model has lower bias and RMSE% (-0.05 and 24.67% respectively), which can be attributed to the effectiveness of the LiDAR data to accurately capture branch and leaf biomass (Allouis et al., 2013).

If we compare the results with those of studies carried out in the same forest using single-tree detection methods, it can be observed that the EABA approach resulted in slightly worse biomass estimation accuracy (in both SB and TB) (Georgopoulos et al., 2021). This is attributable to the various co-registration and position errors that can easily occur between the ground and Airborne Laser Scanning (ALS) statistics, which can shift the plot sides in different directions. In the single-tree approach, only clearly detected and identified trees were used, which significantly reduces the estimation errors. The single-tree approach is more computationally demanding compared to the EABA, and results in a minor improvement in terms of biomass estimation accuracy.

In the present work, 48 plots were used for SB and TB estimation, divided into training and testing sets (70% and 30% respectively). Although the number of plots is sufficient for statistical analysis, an increased sample size would provide more reliable estimates. In addition, the model validation and transferability should be tested in a wider range of conditions that are representative of multilayered forests.

Although this research reached its objectives, there are some noteworthy limitations. The models are specifically calibrated for multilayered fir forests with natural regeneration and, as a result, the specific methodology can be transferred only to similar biomes. Furthermore, the research focused primarily on the trees that can be detected in the LiDAR point cloud, excluding all the understorey trees. In addition, only height-derived metrics were employed for the SB and TB estimations, while the intensity metrics were removed. The importance of intensity in biomass estimation has been highlighted in several studies (Dalponte et al., 2018; Hopkinson et al., 2016) and should be studied further.

Overall, the present research shows the ability of multispectral LiDAR data to provide accurate SB and TB estimations in a complex structured forest. This study highlights the importance of height-derived metrics for above-ground biomass estimation, which is crucial for the sustainable and effective management of forest ecosystems.

5 Conclusions

The potential of multispectral LiDAR data to estimate stem and total biomass using the EABA approach was examined. Specifically, a Random Forest regression algorithm and LiDAR-derived height-related metrics were used as inputs to estimate the plot-based predictions of SB and TB. The results demonstrated the capability of multispectral LiDAR data to provide reliable estimates for both stem and total biomass, in a dense, multilayered coniferous forest. More specifically:

- Stem biomass can be adequately predicted using LiDAR-derived height-related metrics and the RF algorithm.
- Total biomass was predicted with higher accuracy than stem biomass; this was the most precise estimation obtained using the RF model.
- The RF algorithm can provide accurate biomass predictions in multilayered stands.
- The height metrics derived from both spectral channels contribute to accurate biomass predictions.

This research offers an approach for estimating above-ground biomass in complex-structured forests where the alternative of field measurements would be extremely costly and laborious. Given the limitations described in Section 4, future work might investigate the difference in accuracy between typical plot-based methods and EABA in similarly complex and dense stands. Another assessment could take into account intensity-related metrics and investigate their capacity to improve estimation accuracy.

References

Allouis, T., Durrieu, S., Vega, C., & Couteron, P. (2013). Stem Volume and Above-Ground Biomass Estimation of Individual Pine Trees From LiDAR Data: Contribution of Full-Waveform Signals. IEEE Journal of Selected Topics in Applied Earth Observations and Remote Sensing, 6(2), 924–934. https://doi.org/10.1109/JSTARS.2012.2211863

Almeida, C. T. de, Galvão, L. S., Aragão, L. E. de O. C. e, Ometto, J. P. H. B., Jacon, A. D., Pereira, F. R. de S., … Longo, M. (2019). Combining LiDAR and hyperspectral data for aboveground biomass modeling in the Brazilian Amazon using different regression algorithms. Remote Sensing of Environment, 232, 111323. https://doi.org/10.1016/j.rse.2019.111323

Cao, L., Coops, N., Innes, J., Dai, J., & She, G. (2014). Mapping Above- and Below-Ground Biomass Components in Subtropical Forests Using Small-Footprint LiDAR. Forests, 5(6), 1356–1373. https://doi.org/10.3390/f5061356

Cao, L., Liu, K., Shen, X., Wu, X., & Liu, H. (2019). Estimation of Forest Structural Parameters Using UAV-LiDAR Data and a Process-Based Model in Ginkgo Planted Forests. IEEE Journal of Selected Topics in Applied Earth Observations and Remote Sensing, 12(11), 4175–4190. https://doi.org/10.1109/JSTARS.2019.2918572

Clark, M. L. (2011). Estimation of tropical rain forest aboveground biomass with small-footprint lidar and hyperspectral sensors. Remote Sensing of Environment, 12.

Coomes, D. A., Dalponte, M., Jucker, T., Asner, G. P., Banin, L. F., Burslem, D. F. R. P., … Qie, L. (2017). Area-based vs tree-centric approaches to mapping forest carbon in Southeast Asian forests from airborne laser scanning data. Remote Sensing of Environment, 194, 77–88. https://doi.org/10.1016/j.rse.2017.03.017

Dalponte, M., Ene, L., Gobakken, T., Næsset, E., & Gianelle, D. (2018). Predicting Selected Forest Stand Characteristics with Multispectral ALS Data. Remote Sensing, 10(4), 586. https://doi.org/10.3390/rs10040586

Dong, L., Tang, S., Min, M., Veroustraete, F., & Cheng, J. (2019). Aboveground forest biomass based on OLSR and an ANN model integrating LiDAR and optical data in a mountainous region of China. International Journal of Remote Sensing, 40(15), 6059–6083. https://doi.org/10.1080/01431161.2019.1587201

Donoghue, D., Watt, P., Cox, N., & Wilson, J. (2007). Remote sensing of species mixtures in conifer plantations using LiDAR height and intensity data. Remote Sensing of Environment, 110(4), 509–522. https://doi.org/10.1016/j.rse.2007.02.032

Dorado-Roda, I., Pascual, A., Godinho, S., Silva, C., Botequim, B., Rodríguez-Gonzálvez, P., … Guerra-Hernández, J. (2021). Assessing the Accuracy of GEDI Data for Canopy Height and Aboveground Biomass Estimates in Mediterranean Forests. Remote Sensing, 13(12), 2279. https://doi.org/10.3390/rs13122279

Dutcă, I., Zianis, D., Petriţan, I. C., Bragă, C. I., Ştefan, G., Yuste, J. C., & Petriţan, A. M. (2020). Allometric Biomass Models for European Beech and Silver Fir: Testing Approaches to Minimize the Demand for Site-Specific Biomass Observations. Forests, 11(11), 1136. https://doi.org/10.3390/f11111136

Georgopoulos, N., Gitas, I. Z., Stefanidou, A., Korhonen, L., & Stavrakoudis, D. (2021). Estimation of Individual Tree Stem Biomass in an Uneven-Aged Structured Coniferous Forest Using Multispectral LiDAR Data. Remote Sensing, 13(23), 4827. https://doi.org/10.3390/rs13234827

Hopkinson, C., Chasmer, L., Gynan, C., Mahoney, C., & Sitar, M. (2016). Multisensor and Multispectral LiDAR Characterization and Classification of a Forest Environment. Canadian Journal of Remote Sensing, 42(5), 501–520. https://doi.org/10.1080/07038992.2016.1196584

Jiang, X., Li, G., Lu, D., Chen, E., & Wei, X. (2020). Stratification-Based Forest Aboveground Biomass Estimation in a Subtropical Region Using Airborne Lidar Data. Remote Sensing, 12(7), 1101. https://doi.org/10.3390/rs12071101

Kajimoto, T., Matsuura, Y., Sofronov, M. A., Volokitina, A. V., Mori, S., Osawa, A., & Abaimov, A. P. (1999). Above- and belowground biomass and net primary productivity of a Larix gmelinii stand near Tura, central Siberia. Tree Physiology, 19(12), 815–822. https://doi.org/10.1093/treephys/19.12.815

Kelley, J., Trofymow, J. A. (Tony), Metsaranta, J. M., Filipescu, C. N., & Bone, C. (2021). Use of Multi-Temporal LiDAR to Quantify Fertilization Effects on Stand Volume and Biomass in Late-Rotation Coastal Douglas-Fir Forests. Forests, 12(5), 517. https://doi.org/10.3390/f12050517

Khosravipour, A., Skidmore, A. K., Isenburg, M., Wang, T., & Hussin, Y. A. (2014). Generating Pit-free Canopy Height Models from Airborne Lidar. Photogrammetric Engineering & Remote Sensing, 80(9), 863–872. https://doi.org/10.14358/PERS.80.9.863

Korpela, I., Hovi, A., & Morsdorf, F. (2012). Understory trees in airborne LiDAR data—Selective mapping due to transmission losses and echo-triggering mechanisms. Remote Sensing of Environment, 119, 92–104. https://doi.org/10.1016/j.rse.2011.12.011

Kotivuori, E., Maltamo, M., Korhonen, L., Strunk, J. L., & Packalen, P. (2021). Prediction error aggregation behaviour for remote sensing augmented forest inventory approaches. Forestry: An International Journal of Forest Research, 94(4), 576–587. https://doi.org/10.1093/forestry/cpab007

Latella, M., Sola, F., & Camporeale, C. (2021). A Density-Based Algorithm for the Detection of Individual Trees from LiDAR Data. Remote Sensing, 13(2), 322. https://doi.org/10.3390/rs13020322

Li, Y., Li, C., Li, M., & Liu, Z. (2019). Influence of Variable Selection and Forest Type on Forest Aboveground Biomass Estimation Using Machine Learning Algorithms. Forests, 10(12), 1073. https://doi.org/10.3390/f10121073

Luo, S., Wang, C., Xi, X., Pan, F., Peng, D., Zou, J., … Qin, H. (2017). Fusion of airborne LiDAR data and hyperspectral imagery for aboveground and belowground forest biomass estimation. Ecological Indicators, 73, 378–387. https://doi.org/10.1016/j.ecolind.2016.10.001

Næsset, E. (2004). Practical large-scale forest stand inventory using a small-footprint airborne scanning laser. Scandinavian Journal of Forest Research, 19(2), 164–179. https://doi.org/10.1080/02827580310019257

Oliver, M. A., & Webster, R. (1990). Kriging: A method of interpolation for geographical information systems. International Journal of Geographical Information Systems, 4(3), 313–332. https://doi.org/10.1080/02693799008941549

Packalen, P., Strunk, J. L., Pitkanen, J. A., Temesgen, H., & Maltamo, M. (2015). Edge-Tree Correction for Predicting Forest Inventory Attributes Using Area-Based Approach With Airborne Laser Scanning. IEEE Journal of Selected Topics in Applied Earth Observations and Remote Sensing, 8(3), 1274–1280. https://doi.org/10.1109/JSTARS.2015.2402693

Pascual. (2019). Using Tree Detection Based on Airborne Laser Scanning to Improve Forest Inventory Considering Edge Effects and the Co-Registration Factor. Remote Sensing, 11(22), 2675. https://doi.org/10.3390/rs11222675

R Core Team. (2017). R: A Language and Environment for Statistical Computing. R Foundation for Statistical Computing. Retrieved from https://www.R-project.org/

Roussel, J.-R., Auty, D., Coops, N. C., Tompalski, P., Goodbody, T. R. H., Meador, A. S., … Achim, A. (2020). lidR: An R package for analysis of Airborne Laser Scanning (ALS) data. Remote Sensing of Environment, 251, 112061. https://doi.org/10.1016/j.rse.2020.112061

Salum, R. B., Souza-Filho, P. W. M., Simard, M., Silva, C. A., Fernandes, M. E. B., Cougo, M. F., … Rogers, K. (2020). Improving mangrove above-ground biomass estimates using LiDAR. Estuarine, Coastal and Shelf Science, 236, 106585. https://doi.org/10.1016/j.ecss.2020.106585

Silva, Carlos A., Hudak, A. T., Vierling, L. A., Loudermilk, E. L., O'Brien, J. J., Hiers, J. K., … Khosravipour, A. (2016). Imputation of Individual Longleaf Pine (Pinus palustris Mill.) Tree Attributes from Field and LiDAR Data. Canadian Journal of Remote Sensing, 42(5), 554–573. https://doi.org/10.1080/07038992.2016.1196582

Silva, Carlos Alberto, Saatchi, S., Garcia, M., Labriere, N., Klauberg, C., Ferraz, A., … Hudak, A. T. (2018). Comparison of Small- and Large-Footprint Lidar Characterization of Tropical Forest Aboveground Structure and Biomass: A Case Study From Central Gabon. IEEE Journal of Selected Topics in Applied Earth Observations and Remote Sensing, 11(10), 3512–3526. https://doi.org/10.1109/JSTARS.2018.2816962

Socha, J., Hawryło, P., Pierzchalski, M., Stereńczak, K., Krok, G., Wężyk, P., & Tymińska-Czabańska, L. (2020). An allometric area-based approach—A cost-effective method for stand volume estimation based on ALS and NFI data. Forestry: An International Journal of Forest Research, 93(3), 344–358. https://doi.org/10.1093/forestry/cpz062

Sun, X., Li, G., Wang, M., & Fan, Z. (2019). Analyzing the Uncertainty of Estimating Forest Aboveground Biomass Using Optical Imagery and Spaceborne LiDAR. Remote Sensing, 11(6), 722. https://doi.org/10.3390/rs11060722

Wallace, A., Nichol, C., & Woodhouse, I. (2012). Recovery of Forest Canopy Parameters by Inversion of Multispectral LiDAR Data. Remote Sensing, 4(2), 509–531. https://doi.org/10.3390/rs4020509

Wang, X., & Jiao, H. (2020). Spatial Scaling of Forest Aboveground Biomass Using Multi-Source Remote Sensing Data. IEEE Access, 8, 178870–178885. https://doi.org/10.1109/ACCESS.2020.3027361

Węgiel, A., & Polowy, K. (2020). Aboveground Carbon Content and Storage in Mature Scots Pine Stands of Different Densities. Forests, 11(2), 240. https://doi.org/10.3390/f11020240

Zhang, L., Shao, Z., Liu, J., & Cheng, Q. (2019). Deep Learning Based Retrieval of Forest Aboveground Biomass from Combined LiDAR and Landsat 8 Data. Remote Sensing, 11(12), 1459. https://doi.org/10.3390/rs11121459

Zhang, Z., Cao, L., & She, G. (2017). Estimating Forest Structural Parameters Using Canopy Metrics Derived from Airborne LiDAR Data in Subtropical Forests. Remote Sensing, 9(9), 940. https://doi.org/10.3390/rs9090940